Advanced International Journal for Research (AIJFR)
E-ISSN: 3048-7641 ● Website: www.aijfr.com ● Email: editor@aijfr.com

Antibacterial Activity of Silica with Copper Oxide Nanocomposite and Its Properties

Christy Sandra Fernando.B[1], Nirmala Jothi[2]

[1]Research Scholar, Department of Physics, Loyola College, Chennai
[2]Assistant Professor, Department of Physics, Loyola College, Chennai

Abstract
Nanomaterials are efficient in their antibacterial characteristics. Metals and metal oxides have significant advantage especially copper oxide is preferred due to its enhanced anticancer and antimicrobial activity. The aim of this research article is to highlight the impact of "silica with copper oxide nanocomposite" for antibacterial properties. Silica is a non-toxic material obtained from its precursor, Tetraethyl orthosilicate (TEOS) and copper oxide was obtained from Copper Nitrate Trihydrate. Both the materials were synthesized by the "hydrothermal" method of nanotechnology. The prepared materials were combined in a solution phase to make it a nanocomposite. The material was tested for its structural properties using X-ray Diffraction (XRD), Field Emission Scanning Electron Microscopy (FESEM) with Energy Dispersive X-ray Analysis (EDAX), High-Resolution Transmission Electron Microscopy (HRTEM) with Selected Area Electron Diffraction (SAED). The particle size was found to be about 66 nm. The functional properties of the nanocomposite were analyzed by Fourier Transform Infrared Spectroscopy (FTIR) and Fourier Transform Raman (FT Raman) Spectroscopy techniques. The optical property of the sample was analyzed by Ultraviolet-Visible (UV) Spectroscopy technique. The band gap was found to be 1.4 eV from Tauc's plot. The surface charge of the material was determined using Zeta potential, which is found to be negative. Finally, the material was tested against three gram-positive bacteria and seven gram-negative bacteria using disc diffusion method. The results revealed that Staphylococcus aureus (11mm), Streptococcus pyogenes (11mm), Enterococcus species (12mm), Escherichia coli (9mm), Pseudomonas aeruginosa (10mm), Proteus species (11mm), Salmonella species (10mm), Klebsiella pneumonia (9mm), Escherichia coli – ATCC 25922 (11mm), and Salmonella typhimurium – ATCC 14028 (11mm). The zone of inhibition was analyzed. The nano composite showed good antibacterial properties for tested bacteria. It can be used as antimicrobial agent.

Keywords: Nanotechnology, Silica, Copper oxide, Antibacterial property.

1. Introduction:

Nanomedicine combines the use of Nanotechnology for Medical field applications which include early diagnosis and treatment of infectious diseases caused by pathogenic bacteria, viruses and fungi, targeted and controlled drug delivery, cancer detection and treatment. Biosensors are used in accurate and rapid detection of diseases and metabolites from the blood and bodily fluids [1]. Nanoparticles loaded with antibiotics improves the treatment efficiency against bacterial infections [2]. Metal nanoparticles are proven effective for wound healing, destruction of bacteria and prevention of infection. Due to their tunable particle size and shape, biodegradability, solubility and penetrability into cells and tissues, metal nanoparticles such as zinc, copper, silver and palladium are used in biomedical applications [3].

Nanomaterials are prepared by “top-down” approaches or “physical” methods such as high-energy Ball Milling technique, Ion Beam Technique, Pulsed Laser Deposition and Physical Vapor Deposition (PVD). The “bottom-up” approaches or “chemical” methods of preparing nanomaterials include Sol-gel, Chemical Vapor Deposition (CVD), Hydrothermal, Microemulsion, Solvothermal decomposition [4]. Some of the nanoparticles prepared from physical, chemical and biological method used for medical field application are polymer-based nanoparticles, carbon-based nanomaterials, quantum dots, nanofilms and nano-capsules [5]. “Hydrothermal” is the method of synthesizing high-quality crystalline materials at higher temperature and pressure using a reactor vessel called “autoclave” [6]. Changing the temperature and pH values during synthesis allows yield of nanostructures at different morphology [7]. Rods, spheres, hexagonal structures are synthesized at different sizes by this method and offers high stability in solutions [8]. Hydrothermally synthesized nanoparticles when used in sensor devices produce good stability and reliability [9]. The reaction temperature, reaction time and pressure maintained allows nucleation and growth of particles with desired structural features and influences the properties of the final product [10]. Silica nanoparticles have small particle size, controllable morphology and its mesoporous structure help in effective drug solubility, circulation in the blood stream, targeted and controlled release of drugs [11]. Silica nanoparticles are highly stable, biologically compatible, highly reactive and so have excellent anti-bacterial and anti-fungal properties [12]. Mesoporous silica nanostructures have controllable pore size between 2 to 20 nm, they are excellent for bio-imaging of cancer cells, bone tissue engineering and repair, drug encapsulation and release characteristics [13]. Mesoporous materials have unique features like controllable morphology, particle and pore size and they are used for medical imaging, treating bacterial infections, identifying cancer biomarkers, biosensing to diagnose diseases [14]. The surface of mesoporous structures is modified and synthesized in different morphologies and porosities to overcome the limitations in drug delivery, bone regeneration and bio-imaging [15].

Different metals and metal oxides are used in specific applications for biomedical field [16]. Copper oxide stands significant and unique compared to other metal oxides. Its activity in destroying bacteria and tumor cells is inevitable and suitable for biomedical applications [17]. Copper as a pure metal or doped and its oxides are used as “antibacterial” agents [18]. Copper oxide was synthesized from copper nitrate as precursor by hydrothermal method were used to inhibit bacterial growth of Streptococcus aureus, Escherichia coli and Pseudomonas aeruginosa and to destroy human leukemia cancer cells. Copper oxides are eco-friendly materials, highly stable and resistant to heat [19]. Thus, copper oxide is a promising material to treat bacterial infections and has cytotoxic effect against cancer cells, and so it has higher potential in biomedical applications [20]. The present study is based on “silica with copper oxide nanocomposite” synthesized by the “hydrothermal” method of nanotechnology and tested for antibacterial properties. The active nanocomposite was characterized by using XRD, FESEM with EDAX, HRTEM with SAED, UV, FTIR, FT Raman and Zeta potential analysis.

2. Materials and Methods:

2.1 Materials

All materials were purchased from Sigma Aldrich. Tetraethyl orthosilicate (TEOS) as silica precursor, Cetyl Trimethyl Ammonium Bromide (CTAB) as cationic surfactant, Ethanol, Sodium hydroxide pellets, Ammonia solution and Copper nitrate trihydrate as chemical precursor for copper oxide were used without further purification.

2.2 Preparation of pure silica nanoparticles

The silica nanoparticles were prepared by hydrothermal method [21]. Tetraethyl orthosilicate was used as precursor to synthesize pure nano silica powder [22]. Initially, 0.1M of Cetyl Trimethyl Ammonium Bromide (CTAB) was prepared. About 25 ml Ethanol was added to the milky white soapy solution. About 2 ml of TEOS was added dropwise and the pH was found to be neutral. An aqueous solution of sodium hydroxide was added drop-wise to bring the pH to 12. The solution was heated at 70°C for 2 hours. The solution was hydrothermally treated at 100°C for 6 hours using a stainless-steel Teflon-lined autoclave. The whitish solution was then filtered using Whatman filter paper and the residue was collected in a petri dish. The sample was allowed to freeze below -20°C for about 18 hours. Then, the sample was transferred to lyophilize at -80°C for 7 hours. White powder of pure nano silica was obtained. Figure 1 shows the synthesis procedure of pure nano-silica.

Figure 1: Synthesis Procedure Of Pure Nano-Silica

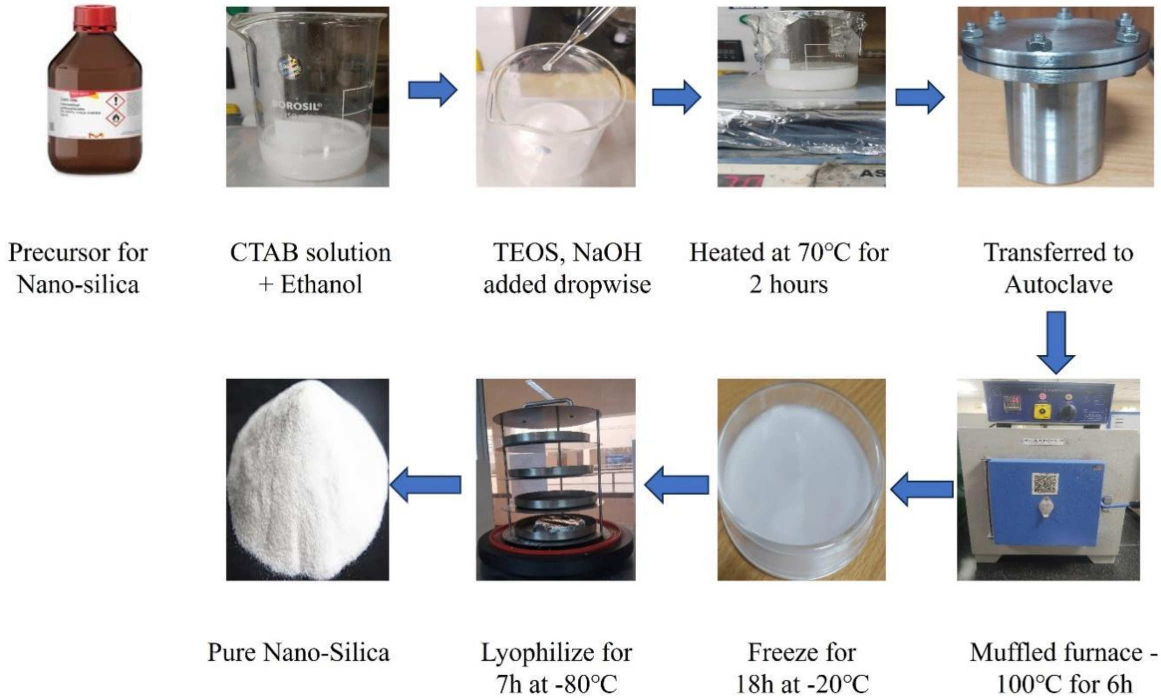

2.3 Preparation of copper oxide nanoparticles

Copper nitrate trihydrate was used as precursor for synthesizing copper oxide nanoparticles [23]. Copper metal oxide was chosen for its notable antibacterial activity [24]. Firstly, 0.5M of copper nitrate solution was prepared by dissolving copper nitrate trihydrate powder in distilled water. Alkaline solution of sodium hydroxide was added dropwise to make the pH equivalent to 12. The solution was heated at 70°C while simultaneously stirring for 2 hours. Color change was observed from blue to bluish green, then black. The solution was transferred to a Teflon-lined stainless-steel autoclave and hydrothermally treated in muffled furnace at 200°C for 6 hours. After reaching room temperature, the solution was filtered and kept in a petri dish. Then it was allowed to freeze at -20°C for 21 hours. It was then lyophilized at -80°C for 7 hours. Finally, black powder of pure copper oxide nanoparticles was obtained. Figure 2 shows the synthesis procedure of pure copper oxide nanoparticles.

Figure 2: Synthesis Procedure of Pure Copper Oxide Nanoparticles

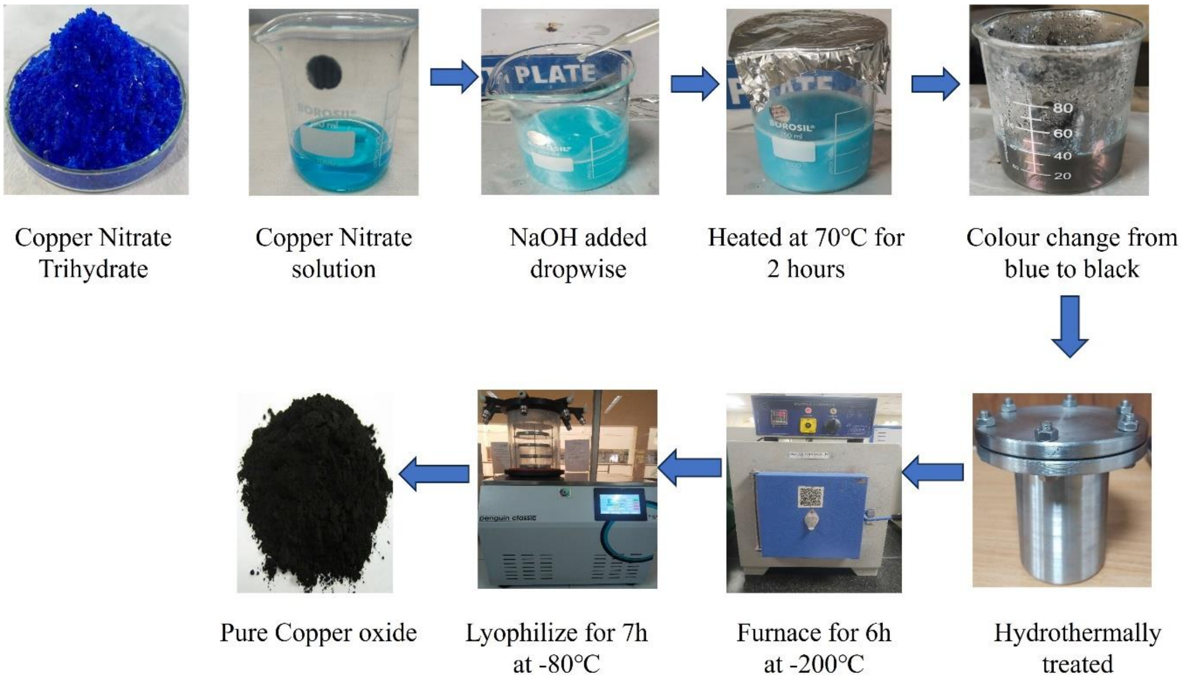

2.4 Preparation of silica with copper oxide nanocomposite

Silica nanoparticles and copper oxide nanoparticles were mixed in a solution to make a nanocomposite of silica with copper oxide [25]. Prepared nano silica powder was mixed with water and ethanol as solvents. Copper oxide nano-powder was mixed with ammonia solution. Both were mixed together and kept in deep freezer at -20°C for 48 hours. Then it was kept to lyophilize at -80°C for 7 hours. Greyish black powder of nano silica with copper oxide was obtained. Figure 3 shows the synthesis procedure of silica with copper oxide nanocomposite.

Figure 3: Synthesis Procedure of Nano-Silica With Copper Oxide Nanocomposite

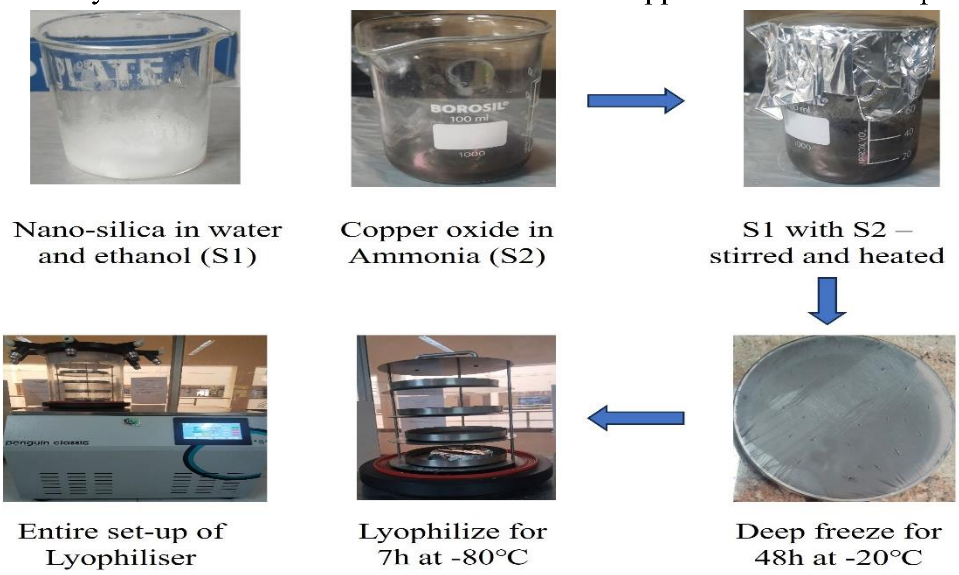

2.5 Antibacterial analysis

2.5.1 Test culture

The bacterial cultures used for testing were obtained from the Department of Microbiology at Ethiraj College, Chennai, India. The Escherichia coli (ATCC 25922) and Salmonella typhimurium strains (ATCC 14028) were procured from Hi-Media Laboratories.

2.5.2 Tested organisms

Three Gram-positive bacteria such as Staphylococcus aureus, Enterococcus species, and Streptococcus pyogenes, were used. Seven Gram-negative bacteria such as Escherichia coli, Escherichia coli (ATCC 25922) strain, Klebsiella pneumoniae, Salmonella species, Pseudomonas aeruginosa, Proteus species, and Salmonella typhimurium (ATCC 14028) strain, were used in the present study.

2.5.3 Preparation of test concentration

The Copper oxide with Nano-Silica is prepared as nano composite and tested against human pathogenic bacteria. The concentration was 1mg/disc concentration.

2.5.4 Inoculum preparation

The bacterial cultures were grown in Muller-Hinton Broth (MHB) at 37 °C for 24h incubation [26]. After incubation, the 24-hour-old culture is ready for an antibacterial susceptibility test. Before starting the test, the inoculum tube was adjusted visually by either adding bacterial colonies if the concentration is too light or by adding sterile normal saline solution if the concentration is too thick. This was done to match the already prepared 0.5 McFarland standard [27], which is assumed to contain a bacterial concentration of 1×10^8 colony-forming unit (CFU)/mL.

2.5.5 Disc diffusion method

Antibacterial activity was carried out using the disc-diffusion method [28]. Petri plates were prepared with 20 ml of sterile Mueller-Hinton Agar (MHA) [29]and made to solidify. About 100µl of bacterial suspension containing 10^8 CFU/ml bacteria were swabbed on the top of the solidified media and allowed to dry for 10 min. The test was conducted at 1 mg/disc concentration each and 25µl/disc for the test sample Copper oxide with Nano-Silica (CS7). The loaded discs were placed on the surface of the agar medium and left for 30 min at room temperature for compounds to diffuse into the medium. Ciprofloxacin (5µg /disc) was used as a positive control (PC) and DMSO - Dimethyl Sulfoxide (25µl/disc) was used as a negative control (NC). The plates were incubated for 24 h at 37°C [30]. After the incubation period, the zone of inhibition (the area around the discs where the bacterial growth was inhibited) was recorded in millimetres.

3. Results and Discussion

Characterization of silica with copper oxide nanocomposite

Silica nanoparticles were synthesized from its precursor Tetraethyl orthosilicate (TEOS), copper oxide nanoparticles were synthesized from its precursor Copper Nitrate Trihydrate. Nanocomposite of silica with copper oxide was prepared by following hydrothermal method of nanotechnology. The nanocomposite “Silica with Copper oxide” was identified for its structural features by X-Ray Diffraction (XRD), Field Emission Scanning Electron Microscopy (FESEM), High-Resolution Transmission Electron Microscopy

(HRTEM) and Selected Area Electron Diffraction (SAED). Origin Software and Image J Software was used in plotting the graphs and finding the particle size and diameter from the FESEM and HRTEM images. The phase of the nanocomposite was observed as monoclinic and crystalline in nature. The crystallite size of the nanocomposite was calculated from Debye-Scherrer equation as 14.56 nm. The micro-strain and dislocation density of the nanocomposite were calculated by Williamson-Hall plot. The morphology of the nanocomposite was found to be spherical. The average diameter was found by Histogram plot as 0.634 nm. The particle size was analyzed by Image J Software as 66.3 nm. The elemental composition of the nanocomposite was identified by Energy Dispersive X-Ray Analysis (EDAX). It confirms the presence of elements silicon, oxygen and copper. The functional groups present in the nanocomposite were identified by Fourier Transform Infra-Red (FTIR) spectroscopy and Fourier Transform Raman (FT Raman) spectroscopy. The optical properties were identified by Ultraviolet-Visible (UV) spectroscopy. The band gap of the nanocomposite was found to be 1.4 eV from Tauc's plot measurement. Zeta potential measurements were done to determine the surface charge of the sample. The nanocomposite exhibited a negative charge. The antibacterial activity was identified for three gram-positive bacteria and seven gram-negative bacteria. The zone of inhibition of the bacteria by the silica with copper oxide nanocomposite was identified.

3.1 X-Ray Diffraction (XRD) of Silica with Copper oxide nanocomposites

Figure 4 shows the X-Ray diffraction spectra of Nano Silicon dioxide (SiO_2) combined with Copper oxide (CuO) prepared by hydrothermal method. (Avg. Crystallite size = 14.56 nm). CuKα radiation was used with wavelength 1.5406 Å [31]. Peaks obtained were in good agreement with JCPDS card no. 96-901-6327 known as Tenorite. The crystal system is monoclinic [32] with C1c1 space group. Sharp peaks obtained shows the crystalline nature of copper oxide with nano silica. Diffraction peaks at 28.83°, 31.96°,35.21°, 38.47°, 48.38°, 53.28°, 57.89°, 61.15°, 65.63°, 67.66°, 72.14° and 74.73° corresponds with miller indices (101), (110), (002), (200), (-202), (020), (202), (-113), (022), (113), (311), (004) respectively. The sharp peak at miller index (200) shows the formation of silica with copper oxide nanocomposite [33].

The crystallite size was found from Debye-Scherrer's equation [34]:

$$D = \frac{k\lambda}{\beta \cos \theta}$$

Where,

k – constant (0.94)

λ – wavelength of X-ray (1.5406 Å)

β – full width half maxima (FWHM)

θ – angle of diffraction

The crystallite size for different peak positions 30.47°, 35.11°, 38.37°, 48.30°, 53.11°, 57.90°, 61.13°, 65.67°, 67.66°, 72° and 74.74° are 7.10 nm, 13.21 nm, 12.79 nm, 13.91 nm, 14.03 nm, 14.01 nm, 14.41 nm, 12.96 nm, 15.12 nm, 23.36 nm and 19.28 nm respectively. The average crystallite size was found to be 14.56 nm.

Figure 4: XRD Pattern Of Silica With Copper Oxide

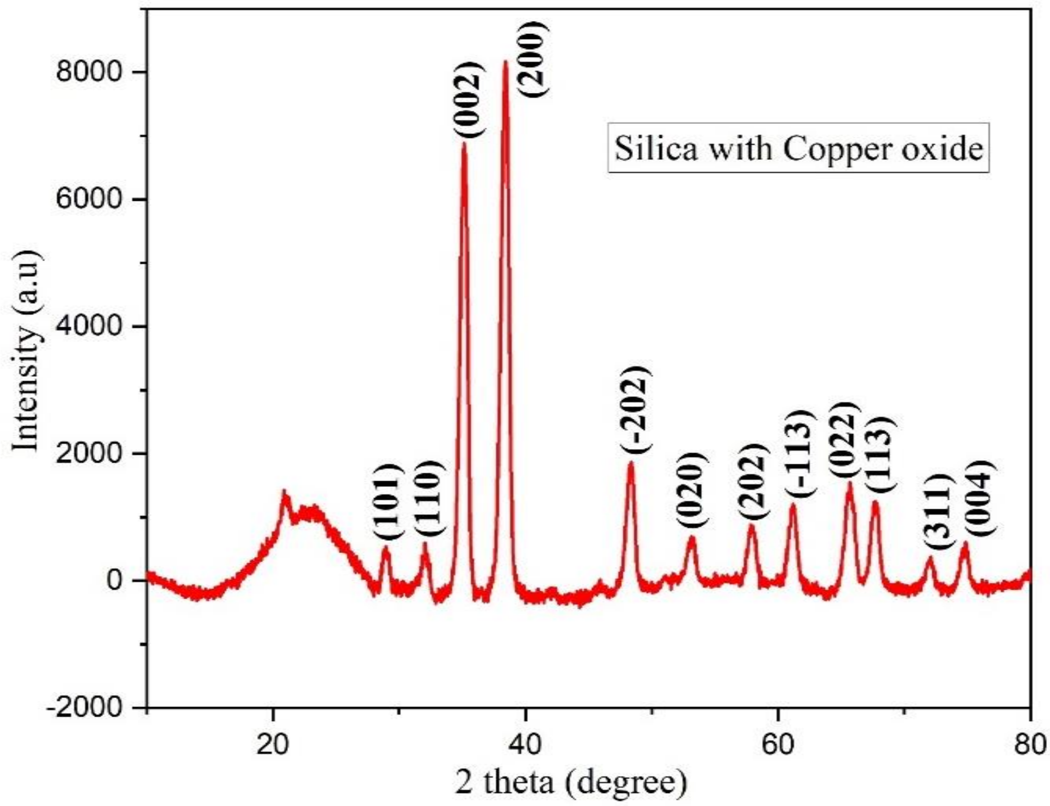

Stress-strain analysis of Silica with Copper oxide:

Figure 5 shows the stress strain plot of copper oxide with nano silica. The micro-strain was calculated from the slope of Williamson-Hall plot shown above by using the formula:

$$\varepsilon = \frac{\beta}{4\, tan\, \theta}$$

Where,

ε – micro-strain in radians/ ratio of peak width to peak position

β – line broadening at FWHM in radians

θ – Bragg's angle in degrees, half of 2θ

The dislocation density was calculated using the formula [35]:

$$\delta = \frac{1}{t^2}$$

Where,

t – crystallite size in nm

The value of micro-strain and dislocation density were found to be 5.62×10^{-3} and 6.0576×10^{-3} respectively.

Figure 5: Micro-strain Plot of Silica With Copper Oxide

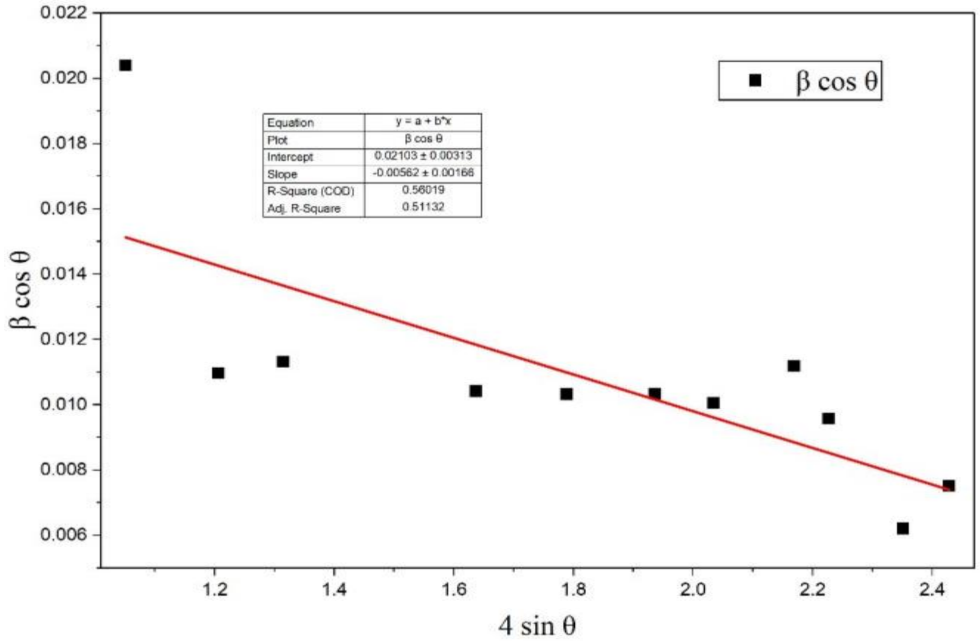

3.2 Field Emission Scanning Electron Microscopy (FESEM) with Energy Dispersive X-Ray Spectroscopy (EDAX)

Figures 6a and 6b show the Field Emission Scanning Electron Microscopy (FESEM) images of Copper oxide with Nano Silica at 0.5 μ-m and 1 μ-m magnifications respectively. The surface morphology of the sample prepared by hydrothermal method was studied under electron microscope [36] at an electrode operating voltage of 15kV [37]. Powder sample was dispersed in ethanol and ultra-sonicated, then coated on an aluminum foil of dimension 1×1 cm and dried before analysis. Images show the nanoflower-like morphology [36] with embedded spherical nanostructures which is due to the presence of silica nanoparticles [38]. The average diameter of particles calculated using ImageJ Software [39] and Origin Software was found to be 0.634 nm which is approximately close to the average crystallite size obtained from X-Ray Diffraction (XRD). The histogram plot obtained for finding the diameter of Copper oxide with Nano Silica nanocomposite is shown in figure 7. The size range of nanoparticles was determined using histogram data [40].

Figures 6a and 6b: Field Emission Scanning Electron Microscopy (FESEM) Image Of Copper Oxide With Nano-Silica At 0.5 μ-m and 1 μ-m Magnifications

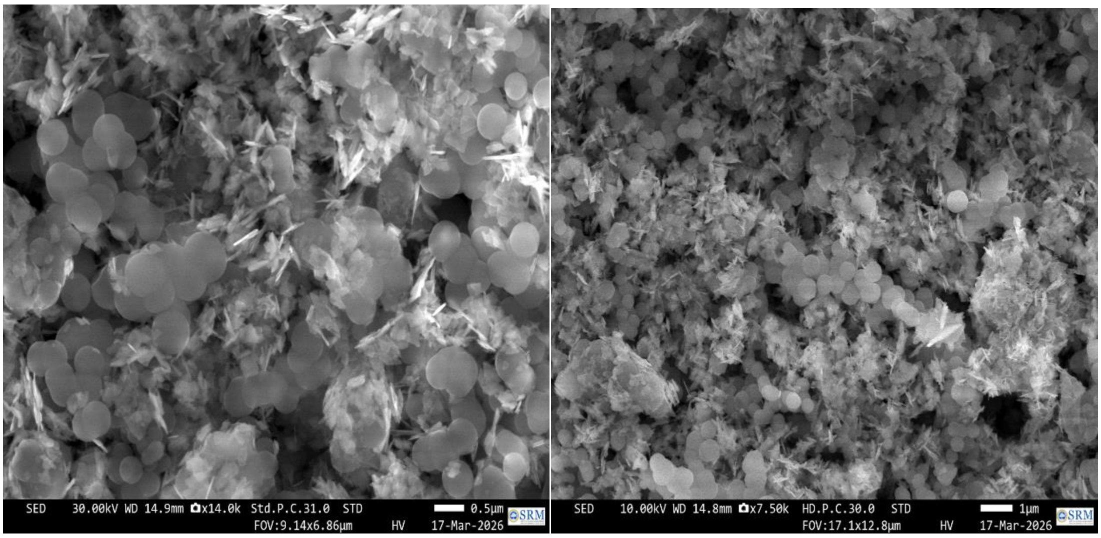

Figure 7: Histogram Plot To Find Diameter

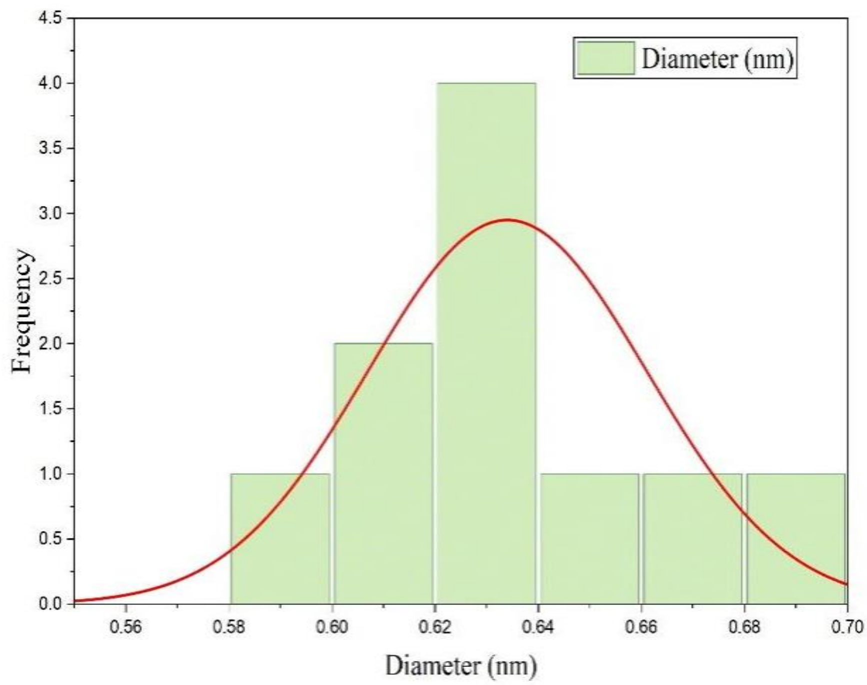

Energy Dispersive X-ray Analysis (EDAX)

Figure 8 shows the Energy Dispersive X-ray Spectrum of Copper oxide with Nano-Silica with Energy in kilo electron volt (keV) on the horizontal axis and Count per second in electron volt (eV) on the vertical axis. To confirm the "elemental chemical composition" of silicon, oxygen and copper, EDAX analysis was performed [41]. Spectra clearly show the peaks of silicon (Si), copper (Cu) and oxygen (O) [42]. In addition to it, carbon (C) is present as impurity. The atomic concentration of Si, Cu and O were 18.32%, 16.66% and 50.79% respectively and the mass concentration of Si, Cu and O were 22.6%, 46.52% and

35.7% respectively. Details of Silica with Copper oxide nanocomposite EDAX spectra values are listed in the table 1.

Figure 8: Elemental Composition

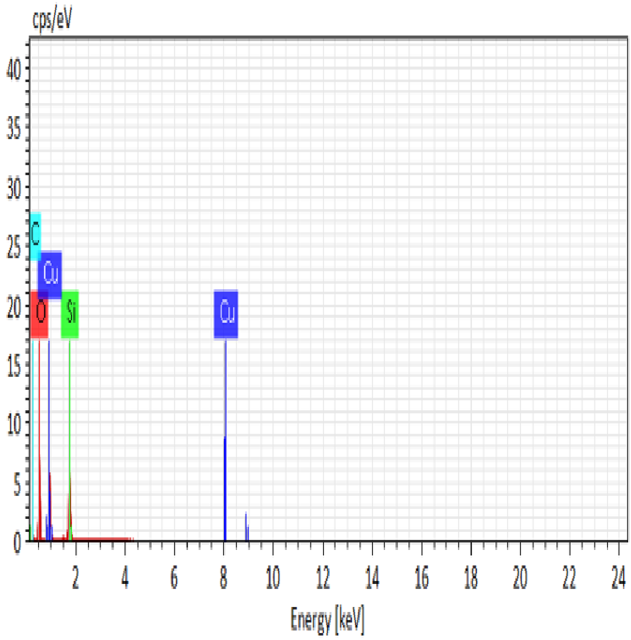

Table 1: Elemental Analysis From EDAX Spectra

Element	Atomic number	Net counts	Mass Concentration /%	Norm. mass concentration /%	Norm. atomic concentration /%	3σ uncertainty /mass%
Cu	29	25089	46.52	41.41	16.66	1.73
O	8	22135	35.70	31.78	50.79	1.53
Si	14	24998	22.60	20.12	18.32	3.11
C	6	1713	7.51	6.69	14.23	0.77
		Sum	**112.33**	**100.00**	**100.00**	

3.3 High-Resolution Transmission Electron Microscopy (HRTEM) with Selected Area Electron Diffraction (SAED) analysis

Figures 9a and 9b show the highly magnified internal microstructures of Copper oxide with Nano-Silica at magnification 100 nm and 500 nm, prepared by hydrothermal method using TEOS precursor and CTAB as surfactant. Ethanol was used to suspend the particles and the solution was dropped in coated grids, dried and viewed under microscope with accelerating voltage 200 kV [43]. Transmission Electron Microscopy images at high resolution indicate the formation of spherical nanoparticle with embedded platelet-like structures in 100 nm image and cluster-like spherical nanoparticles in 500 nm image [44]. The average particle size was found using ImageJ Software as 66.3 nm [45]. Higher particle size is due to the agglomeration of spherical nanostructures [46].

Figures 9a And 9b: High-Resolution Transmission Electron Microscopy Images Of Copper Oxide With Nano-Silica At Magnification 100 nm And 500 nm

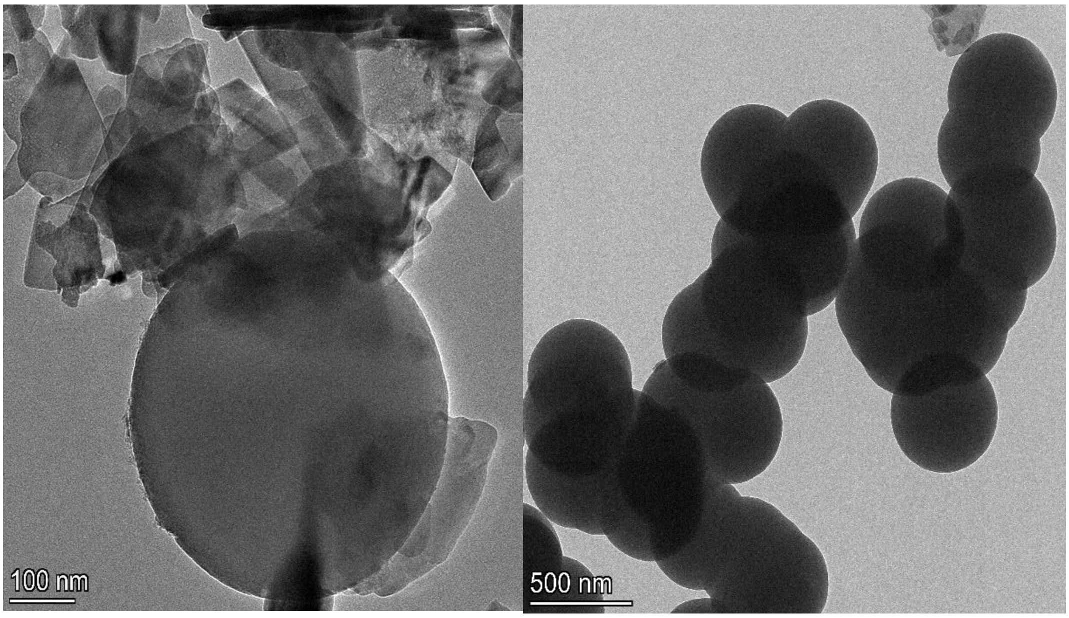

Selected Area Electron Diffraction (SAED)

Figure 10a and 10b shows the SAED pattern of Copper oxide with Silica nanocomposite. To display the accurate local crystal structure of Copper oxide with Nano-Silica, SAED analysis was done at 5 nm^{-1} magnification. Pattern shows discrete spots in ring-like pattern which indicate that the internal structure of nanocomposite is polycrystalline in nature. The d-spacing values in Å were found to be 2.32, 1.36 and 0.918 which corresponds to miller indices (202), (113) and (322) respectively and are indexed in the figure shown. The crystalline plane of copper oxide is approximately indicated in (113) miller index [46]. The miller index at (202) indicates the presence of "Tenorite" a copper oxide mineral in monoclinic phase [47]. By comparing the d-spacing values obtained from XRD and SAED, rings that exist at (202) and (113) strongly indicate the presence of Copper oxide with Silica nanocomposite.

Figure 10a And 10b: Selected Area Electron Diffraction (SAED) Pattern Images Of Copper Oxide With Nano-Silica

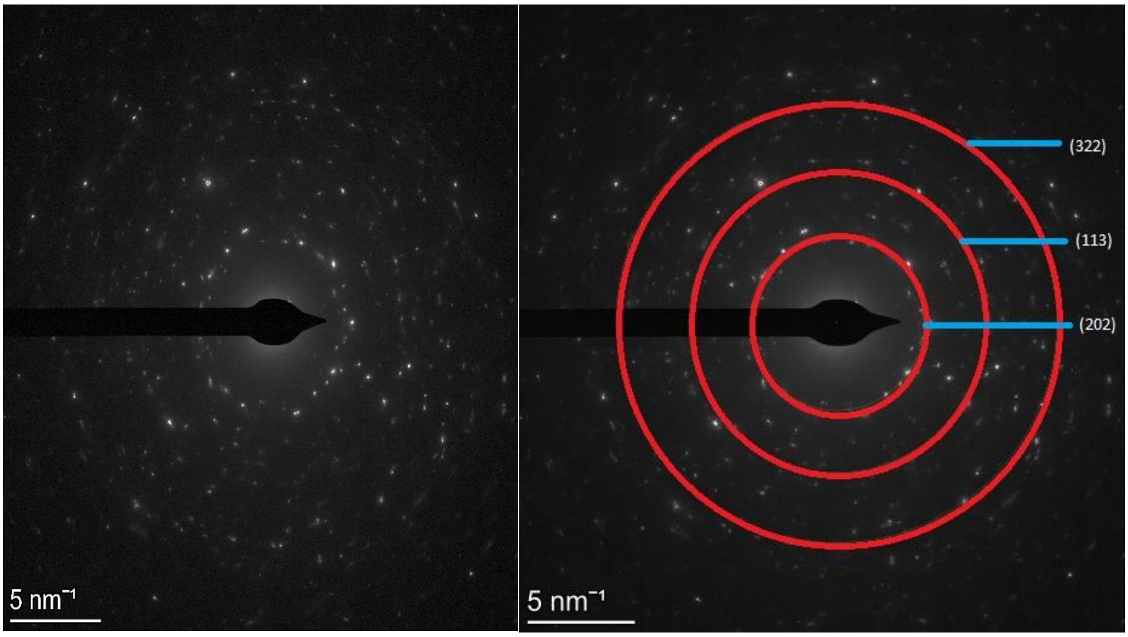

3.4 Ultraviolet-Visible (UV-Vis) Spectroscopy

Figure 11 shows the UV spectrum and Tauc's plot of Copper oxide with Nano-silica. Tauc's plot is used to find the optical band gap of materials [48]. UV-Visible spectrum is plotted with wavelength on the x-axis, absorbance, reflectance or transmittance on the y-axis depending on the nature of the material [49]. Energy band gap reveals the electrical properties of the material [50]. Tauc's plot is done using Origin software by smoothening the curve, baseline correction and determining the accurate band gap value [51]. Optical absorbance spectra of Copper oxide with Nano-silica were recorded in the wavelength region from 200 to 800 nm [52]. A strong absorption is found around 200 nm [53]. From the absorbance spectra, optical band gap energy of Copper oxide with Nano-silica were calculated by Tauc's relation [54]:

$$\alpha h\gamma = B(h\gamma - E_g)^n$$

Where $h\gamma$ – incident photon energy

α – absorption coefficient

B – constant

E_g – band gap of the material

n – depends on the type of the transition for direct band gap materials

Optical band gap was calculated by extrapolating a line on the linear part of the curve intercepting the X-axis ($h\gamma$ in eV) [48]. The observed band gap energy from the Tauc's plot is found to be 1.4 eV.

Figure 11: UV Spectrum And Tauc's Plot

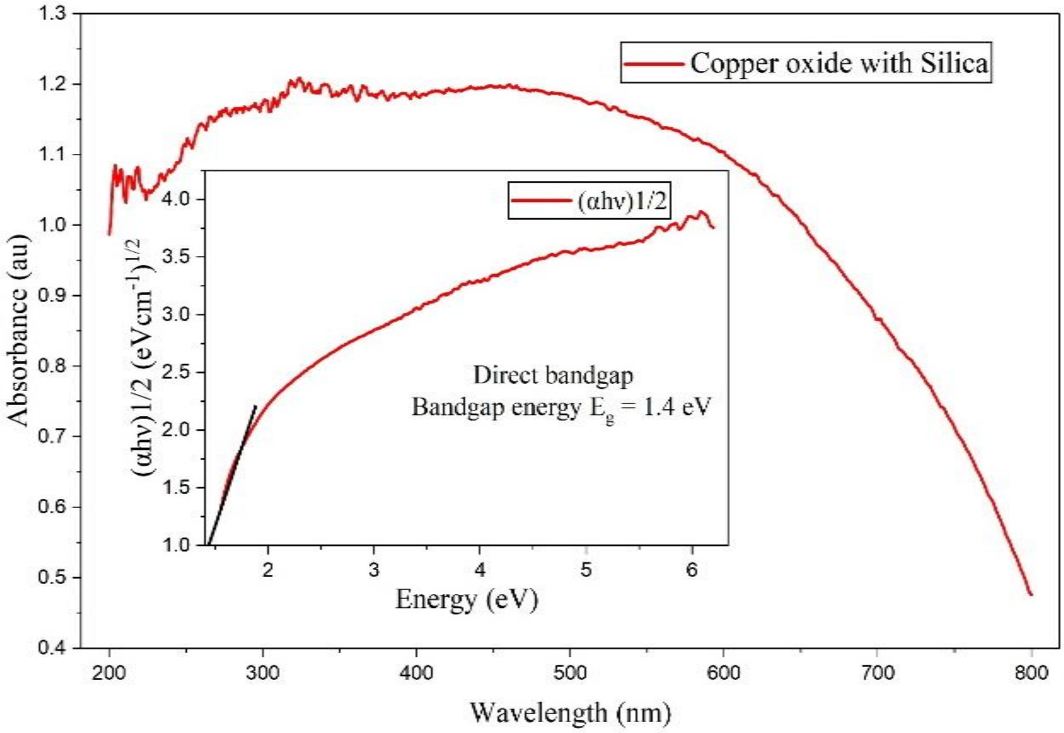

3.5 Fourier Transform Infrared Spectroscopy (FTIR)

Figure 12 shows the Fourier Transform Infrared (FTIR) Spectrum of copper oxide with nano-silica. The functional groups were identified within the wavenumber range from 4000 cm^{-1} to 400 cm^{-1} using Shimadzu IR Tracer-100 FTIR spectrometer [55]. FTIR analysis was performed at room temperature with an instrument measuring both mid and far IR regions [56]. FTIR spectrum is basically plotted with wavenumber in cm^{-1} on the x-axis and transmittance in % on the y-axis [57]. The main peak at 449 cm^{-1} corresponds to inorganic metal-oxygen M-O stretching group and confirms the presence of copper II oxide [58]. The peaks at 1062 cm^{-1} and 802 cm^{-1} which corresponds to C-O stretching and C=C bending vibrations, indicate the bending vibration and asymmetric stretching vibration of silicon and oxygen bonds respectively [59].

Figure 12: FTIR Spectrum Of Nanocomposite

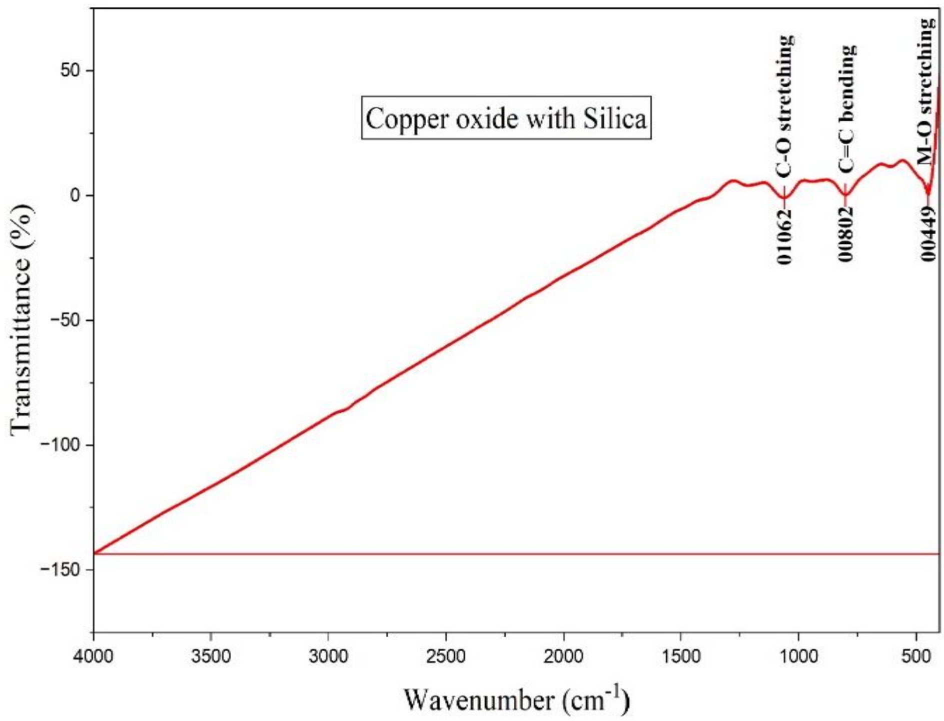

3.6 Fourier Transform Raman Spectroscopy (FT Raman)

Figure 13 shows the Fourier Transform Raman Spectroscopy (FT Raman) graph of Copper oxide with Nano-Silica. To evaluate the structural properties and phase composition of the material, Raman spectroscopy analysis was done [60]. The oxidation states of copper oxide are found using Raman spectroscopy technique [61]. The peak at 611 cm^{-1} corresponds to a class of halo compound with C-Br stretching group which indicates the formation of copper oxide in monoclinic phase [62]. The peaks at 667 cm^{-1}, 739 cm^{-1} and 831 cm^{-1} corresponds to a class of aromatic substitution with C-H out-of-plane bending group. The peak at around 667 cm^{-1} is attributed to the longitudinal mode of Cuprous oxide [63]. The peaks at 1142 cm^{-1} and 1176 cm^{-1} correspond to amorphous sp3 carbon-rich, diamond-like class of compounds. The peak at 1202 cm^{-1} corresponds to a class of alkyl aryl ether with C-O stretching group. The strong and sharp peak at 1325 cm^{-1} corresponds to a class of sulfone with S=O stretching group. Raman spectra at higher wavenumbers indicates copper oxides good for device fabrication applications [64].

Figure 13: FT Raman Spectrum Of Nanocomposite

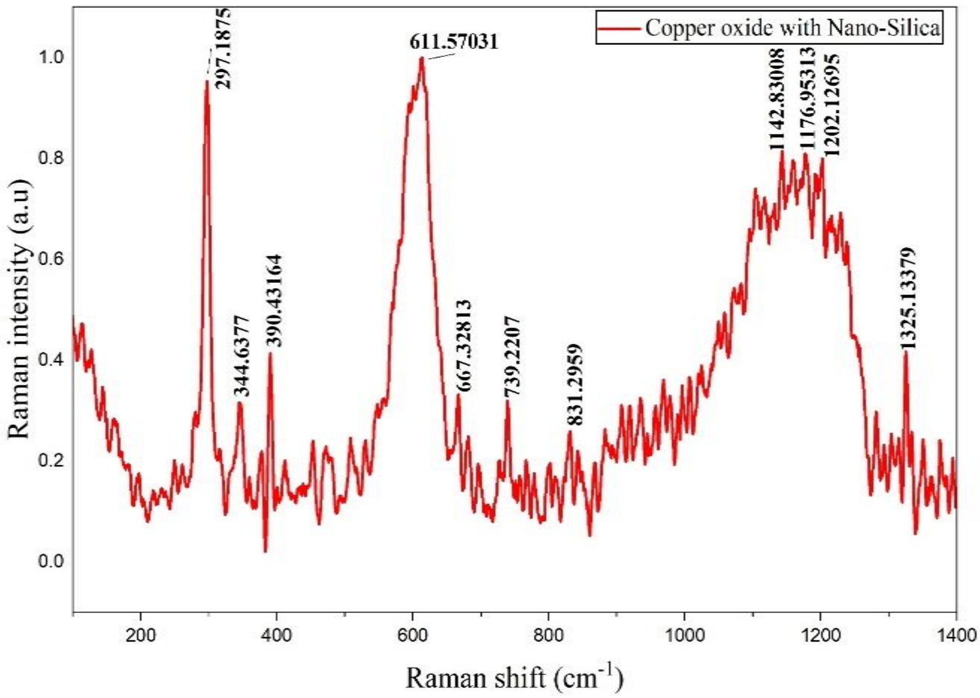

3.7 Zeta potential

Figure 14 shows the zeta potential graph of Copper oxide with Nano-silica. Zeta potential measurements were taken from Horiba Scientific SF-100 to determine the surface charge of the sample [65]. As the surface charge increases, the stability of the sample increases [66]. Zeta potential influences the structure of silica with copper oxide nanocomposite, tailoring the pH values have an impact on their morphology [67]. The surface charge was analyzed using a Temperature of the Holder 25℃, Dispersion Medium Viscosity 0.894 mPa-s, Conductivity 0.104 mS/cm and Electrode Voltage 3.4V. Analysis was taken after powder sample was dispersed in a suitable solvent, dissolved thoroughly and filtered using syringe filter [68]. The charge of the sample's surface was found to be negative [69,70] with a Mean Zeta Potential value -25.3 mV and Mean Electrophoretic Mobility -1.96 × 10^{-4} cm^2/Vs, zeta potential is found from mobility using the "Helmholtz-Smoluchowski equation" [71].

Figure 14: Zeta Potential Graph Of Silica With Copper Oxide

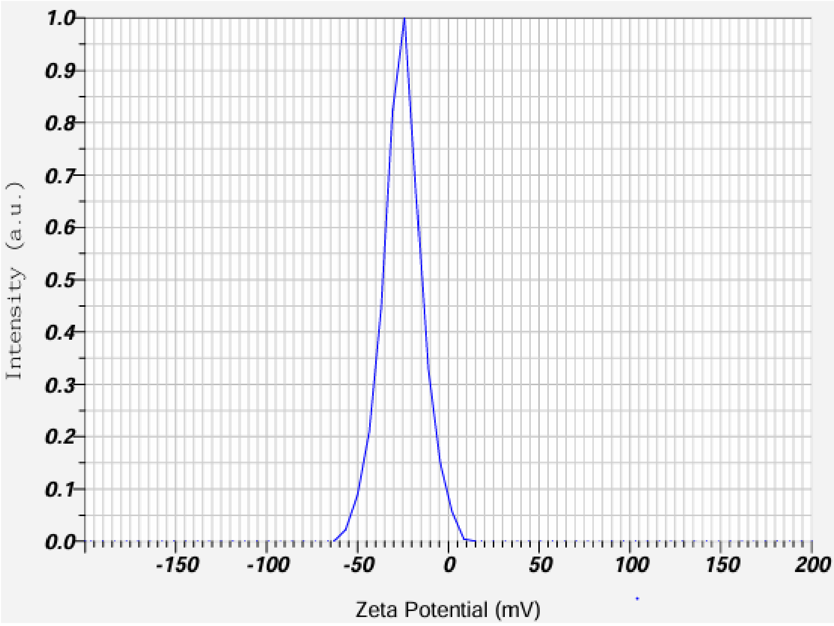

Antibacterial Results

Figures 15a to 15j show the antibacterial activity, the zone of inhibition of ten bacterial species by Copper oxide with Silica nanocomposite. The results of antibacterial activity revealed that the samples at 1 mg/disc were tested against gram-positive and gram-negative pathogenic microorganisms.

Copper oxide with Nano-Silica showed antibacterial activity against gram-positive bacteria such as Staphylococcus aureus (11mm) [72], Streptococcus pyogenes (11mm), Enterococcus species (12mm), and gram-negative bacteria such as Escherichia coli (09mm) [72], Pseudomonas aeruginosa (10mm) [73], Proteus species (11mm), Salmonella species (10mm), Klebsiella pneumonia (09mm) [74], Escherichia coli - 25922 (11mm), and Salmonella typhimurium - 14028 (11mm) at 1 mg/disc. Staphylococcus aureus exhibited the maximum bacterial inhibition efficiency with copper oxide nanoparticles which is greater than other bacterial strains including Escherichia coli and Klebsiella pneumoniae [75].
Ciprofloxacin 5µg/disc was used as a standard control (PC), and Dimethyl Sulfoxide (DMSO) 25µl/disc was used as the negative control (NC).

Figures 15a – 15j: Antibacterial Activity Of Copper Oxide With Silica Nanocomposite On Different Bacteria

Staphylococcus aureus

Streptococcus pyogenes

Enterococcus species

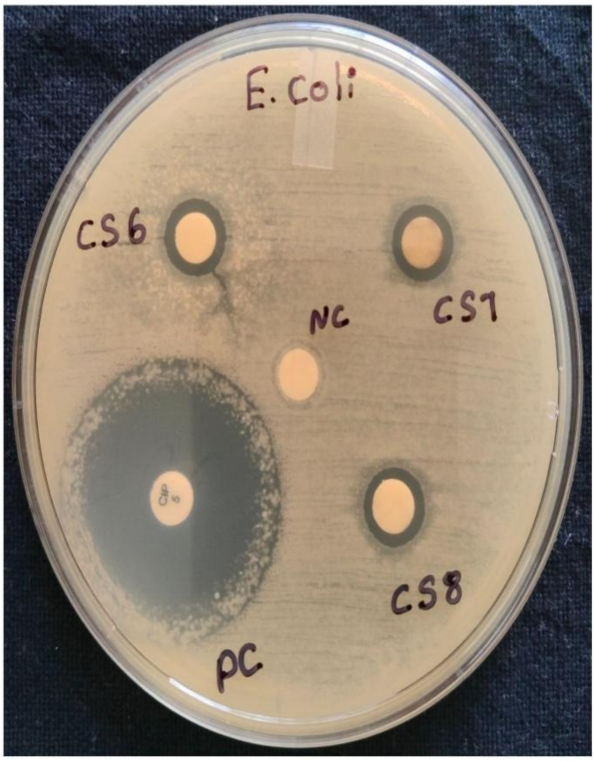

Escherichia coli

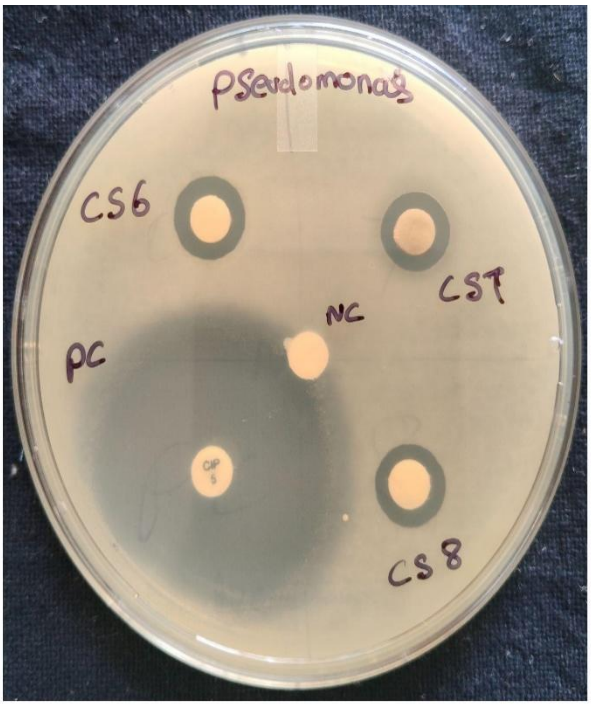

Pseudomonas aeruginosa

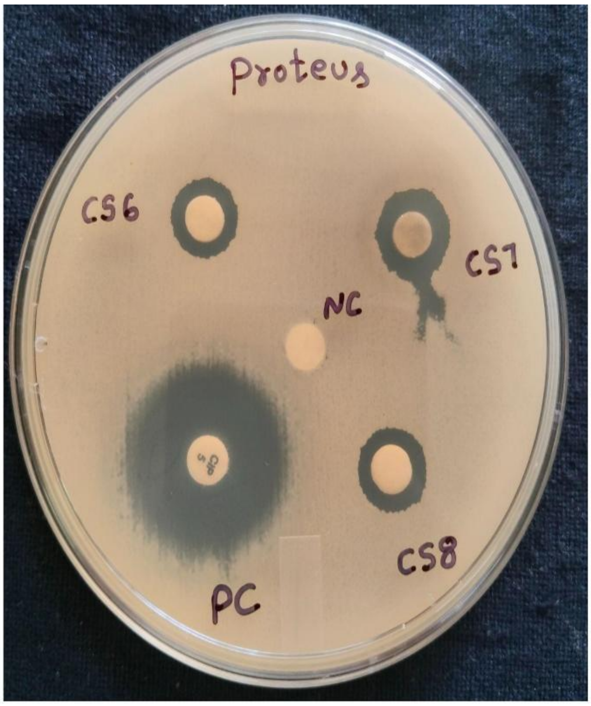

Proteus species

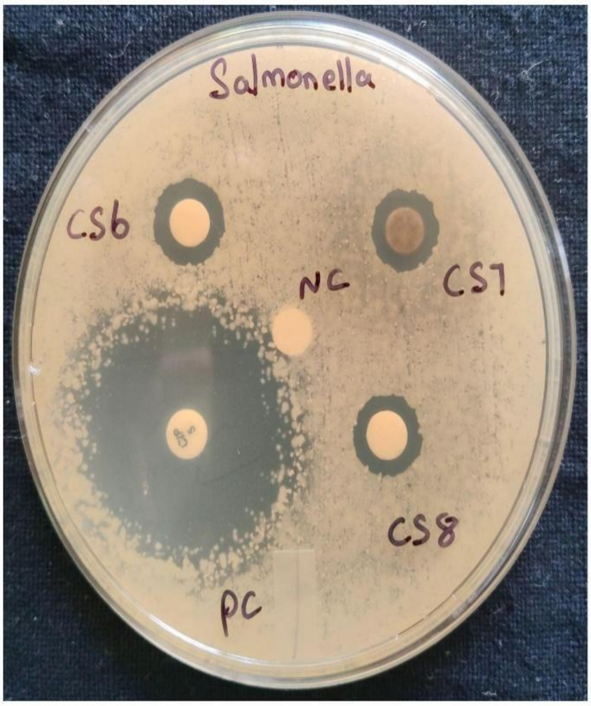

Salmonella species

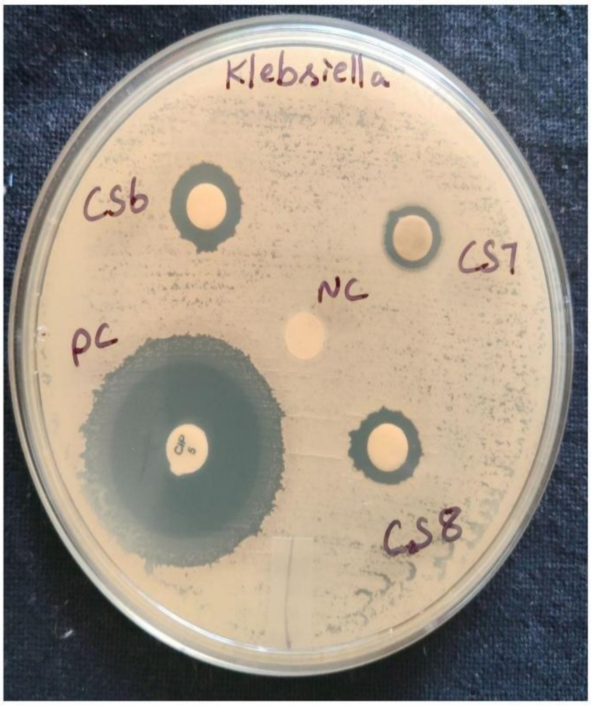

Klebsiella pneumoniae

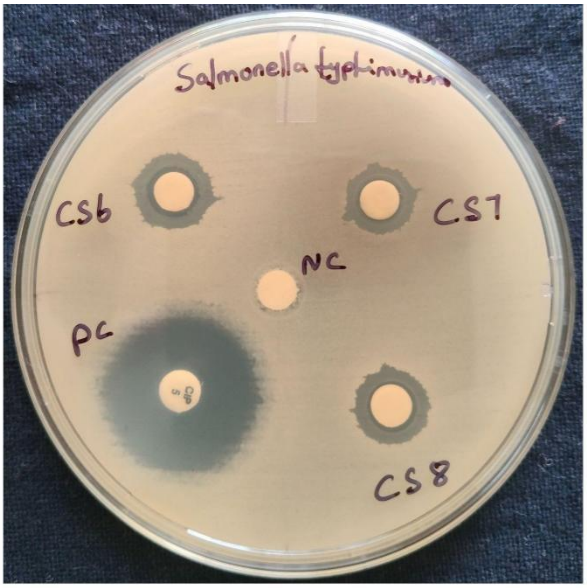

Salmonella typhimurium - 14028

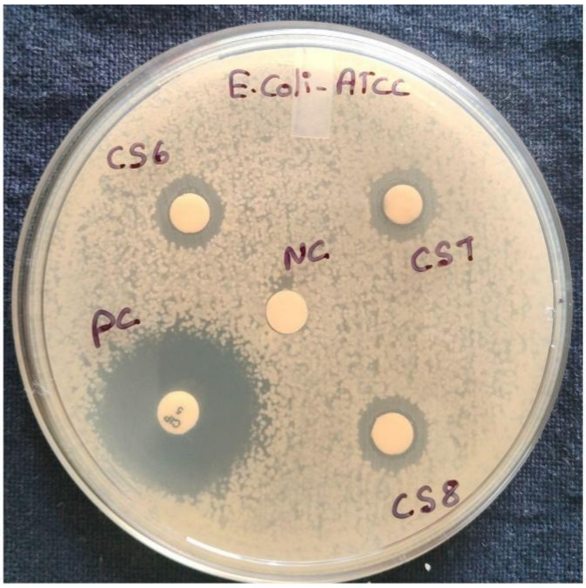

Escherichia coli - 25922

Conclusion:

Nano-silica was synthesized from its precursor Tetraethyl orthosilicate (TEOS), with Cetyl Trimethyl Ammonium Bromide (CTAB) as surfactant with distilled water and ethanol as solvents. Hydrothermal route was used to prepare these nanoparticles, then lyophilized to form crystalline nanoparticles. Then copper oxide was synthesized from its precursor Copper Nitrate Trihydrate using the same hydrothermal procedure. It was also lyophilized and black copper oxide nanoparticles were obtained which was also crystalline in nature. Both the nanoparticles were dissolved in suitable solvents and they were combined in a solution to form nanocomposite of "Silica with Copper oxide". Then, the morphological and structural properties were identified by X-Ray Diffraction (XRD), Field Emission Scanning Electron Microscopy (FESEM), High-Resolution Transmission Electron Microscopy (HRTEM) and Selected Area Electron Diffraction (SAED). The elemental analysis and chemical composition of the sample was identified by Energy Dispersive X-ray Analysis (EDAX). The functional groups present in the sample were determined by Fourier Transform Infrared Spectroscopy (FTIR) and Fourier Transform Raman (FT Raman) Spectroscopy. The optical band gap was identified from Ultraviolet-Visible (UV-Vis) Spectroscopy. Finally, the antibacterial properties of copper oxide were found from "Disc-diffusion method". The zone of inhibition of three gram-positive bacteria and seven gram-negative bacteria were identified. Thus, silica with copper oxide nanocomposite was proved to be an efficient nanocomposite against pathogenic bacteria.

Suggestions for Future work:

Different metals like silver, gold, zinc, magnesium, palladium and platinum are found useful in different biomedical applications including drug delivery, cancer diagnosis and therapy, nano-biosensors for diagnosing diseases, etc. Several metal oxides like zinc oxide, nickel oxide, manganese oxide are found useful for biomedical applications. Carbon-based, polymer materials – In addition to it, carbon-based and polymeric nanomaterials are efficient. Green synthesis from plant parts or bacterial strains are advantageous as they are eco-friendly and does not pollute the environment. Drug encapsulation and release characteristics can be done to find the efficiency of the biomaterial in drug delivery. Cytotoxicity with cancer cell lines can be performed to find the inhibition efficiency of nanocomposites against different types of cancer cells.

Conflicts of Interest:
All authors declare no potential conflict of interest.

References:

1. Abbas, S. F., Haider, A. J., Al-Musawi, S., & Selman, M. K. (2024). Antibacterial Effect of Copper Oxide Nanoparticles Prepared by Laser Production in Water Against Staphylococcus aureus and Escherichia coli. Plasmonics, 19(5), 2401–2411. https://doi.org/10.1007/s11468-023-02135-x
2. Al- Ajeeli, A. F. H., Razeg, K. H., & Fuad Tariq, I. (2023). Copper At Silica Core - Shell Nanoparticles As Antibacterial Agents By Sol-Gel Chemical Methods. 3C Tecnología_Glosas de Innovación Aplicadas a La Pyme, 12(01), 337–352. https://doi.org/10.17993/3ctecno.2023.v12n1e43.337-352
3. Al-Abboodi, S. M. T., Al-Shaibani, E. J. A., & Alrubai, E. A. (2020). Preparation and Characterization of Nano silica Prepared by Different Precipitation Methods. IOP Conference Series: Materials Science and Engineering, 978(1). https://doi.org/10.1088/1757-899X/978/1/012031
4. Al-Jumaili, B. E. B., Talib, Z. A., Ramizy, A., Aljameel, A. I., Baqiah, H., Ahmed, N. M., Paiman, S. B., Liew, J. Y. C., & Lee, H. K. (n.d.). FORMATION AND PHOTOLUMINESCENCE PROPERTIES OF POROUS SILICON/COPPER OXIDE NANOCOMPOSITES FABRICATED VIA ELECTROCHEMICAL DEPOSITION TECHNIQUE FOR PHOTODETECTOR APPLICATION. In Digest Journal of Nanomaterials and Biostructures (Vol. 16, Number 1).
5. Andualem, W. W., Sabir, F. K., Mohammed, E. T., Belay, H. H., & Gonfa, B. A. (2020a). Synthesis of copper oxide nanoparticles using plant leaf extract of catha edulis and its antibacterial activity. Journal of Nanotechnology, 2020. https://doi.org/10.1155/2020/2932434
6. Andualem, W. W., Sabir, F. K., Mohammed, E. T., Belay, H. H., & Gonfa, B. A. (2020b). Synthesis of copper oxide nanoparticles using plant leaf extract of catha edulis and its antibacterial activity. Journal of Nanotechnology, 2020. https://doi.org/10.1155/2020/2932434
7. Ashour, M. M., Mabrouk, M., Soliman, I. E., Beherei, H. H., & Tohamy, K. M. (2021). Mesoporous silica nanoparticles prepared by different methods for biomedical applications: Comparative study. IET Nanobiotechnology, 15(3), 291–300. https://doi.org/10.1049/nbt2.12023
8. Basak, M., Rahman, M. L., Ahmed, M. F., Biswas, B., & Sharmin, N. (2022). The use of X-ray diffraction peak profile analysis to determine the structural parameters of cobalt ferrite nanoparticles using Debye-Scherrer, Williamson-Hall, Halder-Wagner and Size-strain plot: Different precipitating agent approach. Journal of Alloys and Compounds, 895. https://doi.org/10.1016/j.jallcom.2021.162694
9. Bawaked, S., & Narasimharao, K. (2020). Structural and catalytic properties of copper silicate nanomaterials. Scientific Reports, 10(1). https://doi.org/10.1038/s41598-020-57502-z
10. Beisl, S., Herrera Díaz, R., Maroušek, J., Maroušková, A., Periakaruppan, R., Gokul, G. M., Anbukumaran, A., Bohatá, A., Kříž, P., Bárta, J., Pavelčerný, P. P., & Olšan, P. (2022). Silica Nanoparticles from Coir Pith Synthesized by Acidic Sol-Gel Method Improve Germination Economics. https://doi.org/10.3390/polym

11. Benhadria, N., Hachemaoui, M., Zaoui, F., Mokhtar, A., Boukreris, S., Attar, T., Belarbi, L., & Boukoussa, B. (2022). Catalytic Reduction of Methylene Blue Dye by Copper Oxide Nanoparticles. Journal of Cluster Science, 33(1), 249–260. https://doi.org/10.1007/s10876-020-01950-0
12. Bezza, F. A., Tichapondwa, S. M., & Chirwa, E. M. N. (2020). Fabrication of monodispersed copper oxide nanoparticles with potential application as antimicrobial agents. Scientific Reports, 10(1). https://doi.org/10.1038/s41598-020-73497-z
13. Biriukov, D., Fibich, P., & Předota, M. (2020). Zeta Potential Determination from Molecular Simulations. Journal of Physical Chemistry C, 124(5), 3159–3170. https://doi.org/10.1021/acs.jpcc.9b11371
14. Bukhari, S. I., Hamed, M. M., Al-Agamy, M. H., Gazwi, H. S. S., Radwan, H. H., & Youssif, A. M. (2021). Biosynthesis of Copper Oxide Nanoparticles Using Streptomyces MHM38 and Its Biological Applications. Journal of Nanomaterials, 2021. https://doi.org/10.1155/2021/6693302
15. Chatterjee, R., Lidin, S., Bhattacharyya, S., & Kuila, S. K. (2021). Structure, microstructure and photocatalytic properties of embedded spherical Cu nanoparticles on Cu2O–SiO2. Materials Chemistry and Physics, 263. https://doi.org/10.1016/j.matchemphys.2021.124360
16. Chauhan, A., Verma, R., Batoo, K. M., Kumari, S., Kalia, R., Kumar, R., Hadi, M., Raslan, E. H., & Imran, A. (2021). Structural and optical properties of copper oxide nanoparticles: A study of variation in structure and antibiotic activity. Journal of Materials Research, 36(7), 1496–1509. https://doi.org/10.1557/s43578-021-00193-7
17. Chen, H., Cui, Y., Liu, X., Zhang, M., Hao, S., & Yin, Y. (2020). Study on depositing SiO2 nanoparticles on the surface of jute fiber via hydrothermal method and its reinforced polypropylene composites. Journal of Vinyl and Additive Technology, 26(1), 43–54. https://doi.org/10.1002/vnl.21714
18. Chen, W., Du, L., & Wu, C. (2020). Hydrothermal synthesis of MOFs. In Metal-Organic Frameworks for Biomedical Applications (pp. 141–157). Elsevier. https://doi.org/10.1016/B978-0-12-816984-1.00009-3
19. DileepKumar, V. G., Sridhar, M. S., Aramwit, P., Krut'ko, V. K., Musskaya, O. N., Glazov, I. E., & Reddy, N. (2022). A review on the synthesis and properties of hydroxyapatite for biomedical applications. In Journal of Biomaterials Science, Polymer Edition (Vol. 33, Number 2, pp. 229–261). Taylor and Francis Ltd. https://doi.org/10.1080/09205063.2021.1980985
20. Dwivedi, P., Samdani, M. S., Khan, A. U., Jatrana, I., Bansod, S., Min, K., Hejaz Azmi, S. N., & Alam, M. (2024). Plant-mediated synthesis, characterization, and evaluation of a copper oxide/silicon dioxide nanocomposite by an antimicrobial study. Nanotechnology Reviews, 13(1). https://doi.org/10.1515/ntrev-2024-0105
21. Ejsmont, A., & Goscianska, J. (2023). Hydrothermal Synthesis of ZnO Superstructures with Controlled Morphology via Temperature and pH Optimization. Materials, 16(4). https://doi.org/10.3390/ma16041641
22. El Nahrawy, A. M., Abou Hammad, A. B., & Mansour, A. M. (n.d.). Preparation and Characterization of Transparent Semiconducting Silica Nanocomposites Doped with P 2 O 5 and Al 2 O 3. https://doi.org/10.1007/s12633-021-00962-3/Published
23. Fatimah, S., Ragadhita, R., Fitria, D., Husaeni, A., Bayu, A., & Nandiyanto, D. (2021). How to Calculate Crystallite Size from X-Ray Diffraction (XRD) using Scherrer Method. https://doi.org/10.17509/ijost.v6ix

24. Gangadhar, L., & Subburaj, S. (2025). Nanotechnology advances for biomedical applications. In Frontiers in Nanotechnology (Vol. 7). Frontiers Media SA. https://doi.org/10.3389/fnano.2025.1639506
25. Grover, A., Bumbrah, G. S., & Das, A. (2025). A pilot study on the effect of time and acidic/basic conditions on the development of intent fingermarks using silica-copper oxide (SiO2/CuO) nanocomposite. Egyptian Journal of Forensic Sciences, 15(1). https://doi.org/10.1186/s41935-025-00424-6
26. Gudkov, S. V., Burmistrov, D. E., Fomina, P. A., Validov, S. Z., & Kozlov, V. A. (2024). Antibacterial Properties of Copper Oxide Nanoparticles (Review). In International Journal of Molecular Sciences (Vol. 25, Number 21). Multidisciplinary Digital Publishing Institute (MDPI). https://doi.org/10.3390/ijms252111563
27. Habeeb, M. A., Oreibi, I., Hamza, R. S. A., & Mamoun, F. (2024). Fabrication and Unraveling the Morphological, Structural, Optical and Dielectric Features of PMMA-SiO2/CuO Promising Ternary Nanostructures for Nanoelectronic and Photonic Applications. Silicon, 16(16), 5947–5960. https://doi.org/10.1007/s12633-024-03131-4
28. Hameed, M. S., Antony, S. D. P., Shanmugam, R., & Raghu, S. (2024). Synthesis and Characterization of Nanosilica-Coated Antibiotics, TAP: A Comprehensive Study Utilizing XRD, EDS, FTIR, SEM, and TEM - Invitro Study. Journal of International Oral Health, 16(5), 386–393. https://doi.org/10.4103/jioh.jioh_40_24
29. Hariyanto, B., Wardani, D. A. P., Kurniawati, N., Har, N. P., Darmawan, N., & Irzaman. (2021). X-ray peak profile analysis of silica by Williamson–Hall and size-strain plot methods. Journal of Physics: Conference Series, 2019(1). https://doi.org/10.1088/1742-6596/2019/1/012106
30. Heryanto, H., Tahir, D., Abdullah, B., Sayyed, M. I., Yunas, J., Masrour, R., & Veeravelan, K. (2025). Fast Fourier Transform Implementation for Determining Band Gap Energy from UV–Vis Spectra as a Fresh Methodology. Arabian Journal for Science and Engineering, 50(1), 533–539. https://doi.org/10.1007/s13369-024-09210-3
31. Hosseinpour, S., Walsh, L. J., & Xu, C. (2020). Biomedical application of mesoporous silica nanoparticles as delivery systems: A biological safety perspective. In Journal of Materials Chemistry B (Vol. 8, Number 43, pp. 9863–9876). Royal Society of Chemistry. https://doi.org/10.1039/d0tb01868f
32. Imoisili, P. E., & Jen, T.-C. (2021). Facile Extraction and Characterization of Silica Nanoparticles from Corn Stalk by Sol-Gel Hydrothermal Methods. IOP Conference Series: Materials Science and Engineering, 1107(1), 012030. https://doi.org/10.1088/1757-899x/1107/1/012030
33. Imoisili, P. E., Nwanna, E. C., & Jen, T. C. (2022). Facile Preparation and Characterization of Silica Nanoparticles from South Africa Fly Ash Using a Sol–Gel Hydrothermal Method. Processes, 10(11). https://doi.org/10.3390/pr10112440
34. Janulevicius, M., Klimkevicius, V., Vanetsev, A., Plausinaitiene, V., Sakirzanovas, S., & Katelnikovas, A. (2020). Controlled hydrothermal synthesis, morphological design and colloidal stability of GdPO4·nH2O particles. Materials Today Communications, 23. https://doi.org/10.1016/j.mtcomm.2020.100934
35. Johannes, A. Z., Pingak, R. K., & Bukit, M. (2020). Tauc Plot Software: Calculating energy gap values of organic materials based on Ultraviolet-Visible absorbance spectrum. IOP Conference Series: Materials Science and Engineering, 823(1). https://doi.org/10.1088/1757-899X/823/1/012030

36. Jubu, P. R., Danladi, E., Ndeze, U. I., Adedokun, O., Landi, S., Haider, A. J., Adepoju, A. T., Yusof, Y., Obaseki, O. S., & Yam, F. K. (2024). Comment about the use of unconventional Tauc plots for bandgap energy determination of semiconductors using UV–Vis spectroscopy. Results in Optics, 14. https://doi.org/10.1016/j.rio.2024.100606
37. Jubu, P. R., Obaseki, O. S., Nathan-Abutu, A., Yam, F. K., Yusof, Y., & Ochang, M. B. (2022). Dispensability of the conventional Tauc's plot for accurate bandgap determination from UV–vis optical diffuse reflectance data. Results in Optics, 9. https://doi.org/10.1016/j.rio.2022.100273
38. Kalaiyan, G., Suresh, S., Prabu, K. M., Thambidurai, S., Kandasamy, M., Pugazhenthiran, N., Kumar, S. K., & Muneeswaran, T. (2021). Bactericidal activity of Moringa oleifera leaf extract assisted green synthesis of hierarchical copper oxide microspheres against pathogenic bacterial strains. Journal of Environmental Chemical Engineering, 9(1). https://doi.org/10.1016/j.jece.2020.104847
39. Kankala, R. K., Han, Y. H., Xia, H. Y., Wang, S. Bin, & Chen, A. Z. (2022). Nanoarchitectured prototypes of mesoporous silica nanoparticles for innovative biomedical applications. In Journal of Nanobiotechnology (Vol. 20, Number 1). BioMed Central Ltd. https://doi.org/10.1186/s12951-022-01315-x
40. Kayalvizhi, S., Sengottaiyan, A., Selvankumar, T., Senthilkumar, B., Sudhakar, C., & Selvam, K. (2020). Eco-friendly cost-effective approach for synthesis of copper oxide nanoparticles for enhanced photocatalytic performance. Optik, 202. https://doi.org/10.1016/j.ijleo.2019.163507
41. Keabadile, O. P., Aremu, A. O., Elugoke, S. E., & Fayemi, O. E. (2020). Green and traditional synthesis of copper oxide nanoparticles—comparative study. Nanomaterials, 10(12), 1–19. https://doi.org/10.3390/nano10122502
42. Khoshnazar, S. M., Asadi, A., Holghoomi, R., & Abdolmaleki, A. (2023). Green Synthesis of Silica Nanoparticles/Nanocomposites for Biomedical Applications: A Narraitive Review. Biochemistry (Moscow) Supplement Series B: Biomedical Chemistry, 17(2), 41–49. https://doi.org/10.1134/S1990750823600085
43. Koohikar, A., & Tajabadi, M. (2025). Antibacterial Drug Delivery System. Journal of Advanced Materials and Technologies, 14(1), 77–88. https://doi.org/10.30501/jamt.2025.520186.1327
44. Kuddus, A., Islam, R., Tabassum, S., Bakar, A., & Ismail, M. (n.d.). Synthesis of Si NPs from River Sand Using the Mechanochemical Process and its Applications in Metal Oxide Heterojunction Solar Cells. https://doi.org/10.1007/s12633-019-00267-6/Published
45. Kumar Yadav, V., Amari, A., Mahdhi, N., Elkhaleefa, A. M., Fulekar, M., & Patel, A. (n.d.). A Novel and Economical Approach for the Synthesis of Short Rod-shaped Mesoporous Silica Nanoparticles from Coal Fly Ash Waste by Bacillus circulans MTCC 6811.
46. Lei, Q., Guo, J., Noureddine, A., Wang, A., Wuttke, S., Brinker, C. J., & Zhu, W. (2020). Sol–Gel-Based Advanced Porous Silica Materials for Biomedical Applications. In Advanced Functional Materials (Vol. 30, Number 41). Wiley-VCH Verlag. https://doi.org/10.1002/adfm.201909539
47. Li, X., Xie, S., Xie, H., Shen, M., Ma, Z., & Liu, H. (2024). Exploring biomedical applications with silver and copper nanotechnology. CMat, 1(2). https://doi.org/10.1002/cmt2.20
48. Liu, J., Yuan, S., Bremmer, A., & Hu, Q. (2024). Convergence of Nanotechnology and Bacteriotherapy for Biomedical Applications. In Advanced Science (Vol. 11, Number 16). John Wiley and Sons Inc. https://doi.org/10.1002/advs.202309295

49. Malik, S., Muhammad, K., & Waheed, Y. (2023). Emerging Applications of Nanotechnology in Healthcare and Medicine. In Molecules (Vol. 28, Number 18). Multidisciplinary Digital Publishing Institute (MDPI). https://doi.org/10.3390/molecules28186624
50. Maliki, M., Ifijen, I. H., Ikhuoria, E. U., Jonathan, E. M., Onaiwu, G. E., Archibong, U. D., & Ighodaro, A. (2022). Copper nanoparticles and their oxides: optical, anticancer and antibacterial properties. In International Nano Letters (Vol. 12, Number 4, pp. 379–398). Springer Science and Business Media Deutschland GmbH. https://doi.org/10.1007/s40089-022-00380-2
51. Mallik, M., Monia, S., Gupta, M., Ghosh, A., Toppo, M. P., & Roy, H. (2020). Synthesis and characterization of Cu2O nanoparticles. Journal of Alloys and Compounds, 829. https://doi.org/10.1016/j.jallcom.2020.154623
52. Manikandan, D. B., Arumugam, M., Veeran, S., Sridhar, A., Krishnasamy Sekar, R., Perumalsamy, B., & Ramasamy, T. (n.d.). Biofabrication of ecofriendly copper oxide nanoparticles using Ocimum americanum aqueous leaf extract: analysis of in vitro antibacterial, anticancer, and photocatalytic activities. https://doi.org/10.1007/s11356-020-12108-w/Published
53. Matei, A., Craciun, G., Romanitan, C., Pachiu, C., & Tucureanu, V. (2023). Biosynthesis and Characterization of Copper Oxide Nanoparticles †. Engineering Proceedings, 37(1). https://doi.org/10.3390/ECP2023-14629
54. Mujahid, M. H., Upadhyay, T. K., Khan, F., Pandey, P., Park, M. N., Sharangi, A. B., Saeed, M., Upadhye, V. J., & Kim, B. (2022). Metallic and metal oxide-derived nanohybrid as a tool for biomedical applications. In Biomedicine and Pharmacotherapy (Vol. 155). Elsevier Masson s.r.l. https://doi.org/10.1016/j.biopha.2022.113791
55. Mursyalaat, V., Variani, V. I., Arsyad, W. O. S., & Firihu, M. Z. (2023). The development of program for calculating the band gap energy of semiconductor material based on UV-Vis spectrum using delphi 7.0. Journal of Physics: Conference Series, 2498(1). https://doi.org/10.1088/1742-6596/2498/1/012042
56. Muthuvel, A., Jothibas, M., & Manoharan, C. (2020). Synthesis of copper oxide nanoparticles by chemical and biogenic methods: photocatalytic degradation and in vitro antioxidant activity. Nanotechnology for Environmental Engineering, 5(2). https://doi.org/10.1007/s41204-020-00078-w
57. Nagarajan, F. C., Kannaiyan, S. K., & Boobalan, C. (2022). A Proficient approach to enhance heat transfer using cupric oxide/silica hybrid nanoliquids. Journal of Thermal Analysis and Calorimetry, 147(10), 5589–5598. https://doi.org/10.1007/s10973-021-10956-3
58. Nahar, B., Chaity, S. B., Gafur, M. A., & Hossain, M. Z. (2023). Synthesis of Spherical Copper Oxide Nanoparticles by Chemical Precipitation Method and Investigation of Their Photocatalytic and Antibacterial Activities. Journal of Nanomaterials, 2023. https://doi.org/10.1155/2023/2892081
59. Nanja, A. F., Focke, W. W., & Musee, N. (2020). Aggregation and dissolution of aluminium oxide and copper oxide nanoparticles in natural aqueous matrixes. SN Applied Sciences, 2(7). https://doi.org/10.1007/s42452-020-2952-4
60. Naseer, M., Ramadan, R., Xing, J., & Samak, N. A. (2021). Facile green synthesis of copper oxide nanoparticles for the eradication of multidrug resistant Klebsiella pneumonia and Helicobacter pylori biofilms. International Biodeterioration and Biodegradation, 159. https://doi.org/10.1016/j.ibiod.2021.105201

61. Nilufa Yeasmin, M., Sultana, M., Siddika, A., Tabassum, S., Ullah, S. M., & Shahriar Bashar, M. (n.d.). Structural, Optical, and Morphological Characterization of Silica Nanoparticles Prepared by Sol-Gel Process.
62. Prajapati, J. P., Das, D., Katlakunta, S., Maramu, N., Ranjan, V., & Mallick, S. (2021). Synthesis and characterization of ultrasmall Cu2O nanoparticles on silica nanoparticles surface. Inorganica Chimica Acta, 515. https://doi.org/10.1016/j.ica.2020.120069
63. Priya, M., Venkatesan, R., Deepa, S., Sana, S. S., Arumugam, S., Karami, A. M., Vetcher, A. A., & Kim, S. C. (2023). Green synthesis, characterization, antibacterial, and antifungal activity of copper oxide nanoparticles derived from Morinda citrifolia leaf extract. Scientific Reports, 13(1). https://doi.org/10.1038/s41598-023-46002-5
64. Publications, C., John, M., Tibbetts, K. M., John, M. G., & Tibbetts, K. M. (2020). VCU Scholars Compass VCU Scholars Compass Controlling the morphology of copper-silica nanocomposites from Controlling the morphology of copper-silica nanocomposites from laser ablation in liquid laser ablation in liquid Downloaded from Downloaded from Controlling the morphology of copper-silica nanocomposites from laser ablation in liquid. https://scholarscompass.vcu.edu/chem_pubs/100
65. Qiu, S., Zhou, H., Shen, Z., Hao, L., Chen, H., & Zhou, X. (2020). Synthesis, characterization, and comparison of antibacterial effects and elucidating the mechanism of ZnO, CuO and CuZnO nanoparticles supported on mesoporous silica SBA-3. RSC Advances, 10(5), 2767–2785. https://doi.org/10.1039/c9ra09829a
66. Qurtam, A. A., Elbatal, I., Nasr, F. A., Elgendy, A. A., El-Sayyad, G. S., & El-Batal, A. I. (2025). Synthesis, characterization, antimicrobial and antibiofilm potential of green copper silicate and zinc silicate nanoparticles: kinetic study and reaction mechanism determination. RSC Advances, 15(33), 27429–27440. https://doi.org/10.1039/d5ra03834k
67. Saad Akl, A. A., & Elhadi, M. (n.d.). ESTIMATION OF CRYSTALLITE SIZE, LATTICE PARAMETER, INTERNAL STRAIN AND CRYSTAL IMPURIFICATION OF NANOCRYSTALLINE Al 3 Ni 20 B x ALLOY BY WILLIAMSON-HALL METHOD. In Journal of Ovonic Research (Vol. 16, Number 5).
68. Sackey, J., Nwanya, A. C., Bashir, A. K. H., Matinise, N., Ngilirabanga, J. B., Ameh, A. E., Coetsee, E., & Maaza, M. (2020). Electrochemical properties of Euphorbia pulcherrima mediated copper oxide nanoparticles. Materials Chemistry and Physics, 244. https://doi.org/10.1016/j.matchemphys.2020.122714
69. Saleem, S., Jabbar, A. H., Jameel, M. H., Rehman, A., Kareem, Z. H., Abbas, A. H., Ghaffar, Z., Razzaq, S. A., Pashameah, R. A., Alzahrani, E., Ng, E. P., & Sapuan, S. M. (2022). Enhancement in structural, morphological, and optical properties of copper oxide for optoelectronic device applications. Nanotechnology Reviews, 11(1), 2827–2838. https://doi.org/10.1515/ntrev-2022-0473
70. Samy, A., Ismail, A. M., & Ali, H. (2023). Environmentally friendly mesoporous SiO2 with mixed fiber/particle morphology and large surface area for enhanced dye adsorption. Journal of Materials Science, 58(4), 1586–1607. https://doi.org/10.1007/s10853-022-08119-2
71. Sathiyavimal, S., Vasantharaj, S., Veeramani, V., Saravanan, M., Rajalakshmi, G., Kaliannan, T., Al-Misned, F. A., & Pugazhendhi, A. (2021). Green chemistry route of biosynthesized copper oxide nanoparticles using Psidium guajava leaf extract and their antibacterial activity and effective removal of industrial dyes. Journal of Environmental Chemical Engineering, 9(2). https://doi.org/10.1016/j.jece.2021.105033

72. Seroka, N. S., Taziwa, R., & Khotseng, L. (2022). Green Synthesis of Crystalline Silica from Sugarcane Bagasse Ash: Physico-Chemical Properties. Nanomaterials, 12(13). https://doi.org/10.3390/nano12132184
73. Sharma, M., Sharma, A., & Majumder, S. (2020). Synthesis, microbial susceptibility and anti-cancerous properties of copper oxide nanoparticles- review. Nano Express, 1(1). https://doi.org/10.1088/2632-959X/ab9241
74. Shehabeldine, A. M., Amin, B. H., Hagras, F. A., Ramadan, A. A., Kamel, M. R., Ahmed, M. A., Atia, K. H., & Salem, S. S. (2023). Potential Antimicrobial and Antibiofilm Properties of Copper Oxide Nanoparticles: Time-Kill Kinetic Essay and Ultrastructure of Pathogenic Bacterial Cells. Applied Biochemistry and Biotechnology, 195(1), 467–485. https://doi.org/10.1007/s12010-022-04120-2
75. Ssekatawa, K., Byarugaba, D. K., Angwe, M. K., Wampande, E. M., Ejobi, F., Nxumalo, E., Maaza, M., Sackey, J., & Kirabira, J. B. (2022). Phyto-Mediated Copper Oxide Nanoparticles for Antibacterial, Antioxidant and Photocatalytic Performances. Frontiers in Bioengineering and Biotechnology, 10. https://doi.org/10.3389/fbioe.2022.820218
76. Talebian, S., Shahnavaz, B., Nejabat, M., Abolhassani, Y., & Rassouli, F. B. (2023). Bacterial-mediated synthesis and characterization of copper oxide nanoparticles with antibacterial, antioxidant, and anticancer potentials. Frontiers in Bioengineering and Biotechnology, 11. https://doi.org/10.3389/fbioe.2023.1140010
77. Thakar, M. A., Saurabh Jha, S., Phasinam, K., Manne, R., Qureshi, Y., & Hari Babu, V. V. (2021). X ray diffraction (XRD) analysis and evaluation of antioxidant activity of copper oxide nanoparticles synthesized from leaf extract of Cissus vitiginea. Materials Today: Proceedings, 51, 319–324. https://doi.org/10.1016/j.matpr.2021.05.410
78. Tomina, V. V., Furtat, I. M., Lebed, A. P., Kotsyuda, S. S., Kolev, H., Kanuchova, M., Behunova, D. M., Vaclavikova, M., & Melnyk, I. V. (2020). Diverse Pathway to Obtain Antibacterial and Antifungal Agents Based on Silica Particles Functionalized by Amino and Phenyl Groups with Cu(II) Ion Complexes. ACS Omega, 5(25), 15290–15300. https://doi.org/10.1021/acsomega.0c01335
79. Tulinski, M., Jurczyk, M. U., Arkusz, K., Nowak, M., & Jurczyk, M. (2025). Nanotechnology for Biomedical Applications: Synthesis and Properties of Ti-Based Nanocomposites. In Nanomaterials (Vol. 15, Number 18). Multidisciplinary Digital Publishing Institute (MDPI). https://doi.org/10.3390/nano15181417
80. Varaprasad, K., López, M., Núñez, D., Jayaramudu, T., Sadiku, E. R., Karthikeyan, C., & Oyarzúnc, P. (2020). Antibiotic copper oxide-curcumin nanomaterials for antibacterial applications. Journal of Molecular Liquids, 300. https://doi.org/10.1016/j.molliq.2019.112353
81. Verki, M. T., Halladj, R., Habibzadeh, S., & Shalmani, F. M. (2025). Crystallization and particle size distribution of hydrothermally synthesized SAPO-34: an experimental and population balance study. Scientific Reports, 15(1). https://doi.org/10.1038/s41598-024-81146-y
82. Willinger, M., Felhofer, M., Reimhult, E., & Zirbs, R. (2021). Method for high-yield hydrothermal growth of silica shells on nanoparticles. Materials, 14(21). https://doi.org/10.3390/ma14216646
83. Yadav, R., & R Attarde, R. (2024). Synthesis and Characterization of Rice-Grain-Shaped Nanostructured Copper Oxide by a Chemical Method. International Journal of Science and Research (IJSR), 13(12), 489–492. https://doi.org/10.21275/sr241204110947

84. Yadav, V. K., Amari, A., Wanale, S. G., Osman, H., & Fulekar, M. H. (2023). Synthesis of Floral-Shaped Nanosilica from Coal Fly Ash and Its Application for the Remediation of Heavy Metals from Fly Ash Aqueous Solutions. Sustainability (Switzerland), 15(3). https://doi.org/10.3390/su15032612
85. Yadav, V. K., Choudhary, N., Ali, D., Alarifi, S., Dwivedi, V., Patel, A., & Fulekar, M. H. (2024). A Novel and Economical Approach for the Fusarium Oxysporum Mediated Myco-Synthesis of Mesoporous Floral-Shaped Silica Nanoparticles from Coal Fly Ash Waste. Particle and Particle Systems Characterization, 41(8). https://doi.org/10.1002/ppsc.202400007
86. Yang, X., Liu, W., Tan, F., Zhang, Z., Chen, X., Liang, T., & Wu, C. (2020). A robust strategy of homogeneously hybridizing silica and Cu3(BTC)2 to in situ synthesize highly dispersed copper catalyst for furfural hydrogenation. Applied Catalysis A: General, 596. https://doi.org/10.1016/j.apcata.2020.117518
87. Yang, Y., Zhang, M., Song, H., & Yu, C. (2020). Silica-Based Nanoparticles for Biomedical Applications: From Nanocarriers to Biomodulators. Accounts of Chemical Research, 53(8), 1545–1556. https://doi.org/10.1021/acs.accounts.0c00280
88. Yousefvand, P., Mohammadi, E., Zhuang, Y., Bloukh, S. H., Edis, Z., Gamasaee, N. A., Zanganeh, H., Mansour, F. N., Heidarzadeh, M., Attar, F., Babadaei, M. M. N., Keshtali, A. B., Shahpasand, K., Sharifi, M., Falahati, M., & Cai, Y. (2021). Biothermodynamic, antiproliferative and antimicrobial properties of synthesized copper oxide nanoparticles. Journal of Molecular Liquids, 324. https://doi.org/10.1016/j.molliq.2020.114693
89. Zaki, M. E. A., Elbatal, I., Al-Habeeb, R. S., El-Sayyad, G. S., & El-Batal, A. I. (2026). Green Synthesis, Characterization and Antifungal Potential of Inorganic Copper-Zinc Silicate Nanoparticles. Journal of Cluster Science, 37(2). https://doi.org/10.1007/s10876-026-02992-6
90. Zare, M., & Moradi, L. (2022). Modification of magnetic mesoporous N-doped silica nanospheres by CuO NPs: a highly efficient catalyst for the multicomponent synthesis of some propellane indeno indole derivatives. RSC Advances, 12(54), 34822–34830. https://doi.org/10.1039/d2ra06221f
91. Zeta potential and TEM - CuO. (n.d.).
92. Zhai, X., Guo, J., Zhang, W., & Yang, D. (2020). Effect of zeta potential on coating morphology of SiO2-coated copper powder and conductivity of copper film. Chemical Papers, 74(7), 2123–2131. https://doi.org/10.1007/s11696-020-01061-0
93. Zhang, Z., & Fan, Z. (2020). Application of magnesium ion doped carbon dots obtained: Via hydrothermal synthesis for arginine detection. New Journal of Chemistry, 44(12), 4842–4849. https://doi.org/10.1039/c9nj06409e